Optimal design of medium-buried pipe with horizontal wells

Zhiwei Wang

School of Architecture and Engineering, Anhui University of Technology, Anhui 243032, China;

Abstract. In this paper, based on the emergence of medium-depth cased buried pipe with horizontal wells, a kind of optimization design for this buried pipe is designed. Firstly, a semi-analytical model and related evaluation indexes are established for the model, and three different schemes are used for simulation and comparison, which are: changing the inner and outer diameters of the buried pipe at the same time, changing the outer pipe diameter while keeping the inner pipe diameter unchanged, and changing the inner pipe diameter while keeping the outer pipe diameter unchanged, which are of great significance for the optimization of the design of the new type of buried pipe. In this paper, the establishment of the model mainly adopts the establishment and discretization of the energy equation of heat transfer and uses Fortran software to realize. Ultimately this paper comprehensively consider its temperature distribution, heat storage capacity and its economic type, can be concluded that the above three options in option two of the investment is relatively small, the temperature enhancement is more significant. The results and conclusions of the optimization are very helpful for the optimal design of this kind of buried pipe.

Keywords: optimization design; Deep geothermal resources; Borehole closed-loop geothermal system; Horizontal wells.

1. Introduction

The utilization of fossil energy can lead to a series of problems, such as global warming, melting glaciers, and rising sea levels, so we need to reduce the use of fossil energy. [1,2] Geothermal energy is one of the most promising renewable energy sources at present, which can help reduce the dependence on fossil energy and thus protect the ecological environment. [3] It consists mainly of shallow geothermal energy and medium-depth geothermal energy. [4] While external geothermal energy has significant limitations and requires a relatively large land area, medium-depth geothermal energy can better utilize underground thermal energy resources and, at the same time, can efficiently utilize underground space and groundwater, which has obvious advantages. [5-7] Therefore, medium and deep geothermal energy is vital in new energy utilization. [8] However, realizing the effective development of geothermal energy requires overcoming many challenges, including the uneven distribution of geothermal resources and the limitations on the use of geothermal resources. [9] To address this concern, a technique known as Deep Bore Heat Exchanger (DBHE) has been developed based on the Ground Source Heat Pump (GSHP) principle. [10-11] This innovative method enables the production of higher outlet water temperatures, facilitating enhanced heat extraction and subsequently improving system efficiency. [12]

Therefore, a great deal of research has been carried out on DBHEs and GSHPs before, which includes the analysis of heat transfer models, heat transfer influencing factors, the establishment of evaluation indexes, objective optimization, etc. [13-16] Lazaros Aresti et al. [17] combining GBHE and GHE with a comparative analysis of each type of GHE, the terms thermal resistance, ground temperature gradient, line source, and column heat source modeling, which have been widely studied, are discussed in detail. Wang et al. [18] established a new semi-analytical heat transfer model for medium-deep cased submerged pipe heat exchangers under the influence of groundwater seepage. Du et al. [19] investigated the adiabatic properties of DBHE inner tubes and their modes, as well as the extent to which the ratio of inner and outer tube diameters affects the heat transfer capacity of DBHE, and concluded that the ratio of inner and outer tube diameters has a small effect on the heat transfer capacity. Asal Bidarmaghz et al. [20] developed a new numerical method to investigate the extent to which natural convection affects the thermal performance of DBHEs in deep aquifers and concluded that higher aquifer permeability has a more significant effect on heat production in DBHEs

with shorter well lengths. Hu [21] used an improved analytical model for vertical well heat exchangers to simulate long-term temperature changes in the geotechnical soil around the heat exchanger under seasonally changing conditions, the effect of groundwater flow rate on the soil around the borehole, and to simulate the temperature changes in the surrounding geotechnical soil under different operating time scenarios. On the other hand, Zou et al. [22] derived the effects of the thermal conductivity of each soil layer, soil temperature, and well length on heat transfer efficiency through experimental data and theoretical analysis, respectively. Wang et al. [23] derived the law of the influence of different groundwater seepage on the heat transfer process of the buried pipe containing groundwater and analyzed the impact on the heat transfer efficiency through experimental data. Huang et al [24] established a numerical heat transfer model of a medium-depth buried pipe heat transfer system and simulated and compared the outlet water temperature and heat loss rate of the buried pipe under different operation and stop ratios.

The above research results show that although previous researchers have conducted a lot of studies on DBHEs and GSHPs, there are few studies on this aspect of buried pipes containing horizontal wells, including their influencing factors and optimization design. In order to fill the gap, based on the results of previous research, this paper proposes an optimization design method for the heat transfer process of buried pipes containing horizontal wells in view of the current status of research on the influence of various factors on the heat transfer process in buried pipes containing horizontal wells. The semi-analytical model of horizontal wells is innovatively established, and its influencing factors are controlled and simulated. Based on the analysis of the influencing factors, the temperature distribution, heat storage capacity, and economy of buried pipes containing horizontal wells are discussed. And the economic analysis is carried out under different influencing factors, and the optimization effect and economy are considered comprehensively. The results of the study are of great significance for the simulation and design of the heat transfer performance of buried pipes containing horizontal wells.

2. Model despription

2.1 Physical model

Figure 1 presents a schematic depiction of the structure of the cased underground pipe with horizontal wells, comprising two main sections: a vertical pipe section and a horizontal pipe section. Both the vertical pipe section and the horizontal pipe section are filled with backfill to stabilize the structure, and there is groundwater seepage around the horizontal pipe section. The heat transfer in the vertical pipe section is by heat conduction only, while the horizontal pipe section has both heat conduction and convection heat transfer. The profile of this buried pipe is shown in Figure 2. Its working principle is fluid from the buried pipe three parts of the inflow, and from 1 part of the outflow, and then through the circulating pump and heat pump to supply the user, the temperature is lowered, and then from the three parts of the inflow, the cycle repeats.
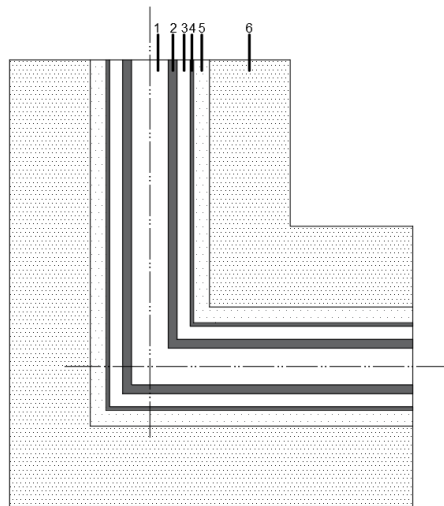
Fig. 1 Schematic Diagram of Underground Pipe System with Horizontal Wells
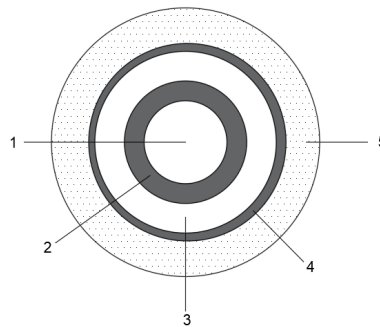
Fig. 2 Schematic Diagram of the section view of Underground Pipe System with Horizontal Wells

2.2 Mathematical model

Table 1 Mathematical model

Nomenclature		h_i	convective heat transfer coefficient of inner pipe fluid(W/(m²·K))
r_{ii}	the inner radius of the inner pipe(m)	λ_{ip}	thermal conductivity of the inner pipe(W/(m·K))
r_{io}	the outer radius of the inner pipe(m)	h_a	convective heat transfer coefficient of the fluid in the outer pipe(W/(m²·K))
$(\rho c)_f$	volumetric specific heat capacity of fluid(J/(m²·K))	$T_{eo}(z,t)$	temperature of the well wall in the vertical pipe section(°C)
$(\rho c)_{ip}$	volumetric specific heat capacity of the inner pipe(J/(m²·K))	R_{ae}	thermal resistance between annular fluid and well wall in vertical tubing section(m·K/W)
$T_{i1}(z,t)$	temperature of the fluid in the inner pipe of the vertical pipe section(°C)	λ_{ep}	thermal conductivity of the outer pipe(W/(m·K))
z	axial coordinates of vertical pipe segments(m)	t_n	the time corresponding to the nth moment(s)
t	times(s)	$T_0(z)$	initial soil temperature(°C)
$V(t)$	volume flow rate of fluid(m³/s)	t_j	the time corresponding to the jth moment(s)
$T_{a1}(z,t)$	temperature of the fluid in the outer pipe of the vertical pipe section(°C)	$T_{in}(t)$	Inlet Fluid Temperature(°C)
L1	length of vertical pipe section heat exchanger(m)	a	land temperature gradient(K/m)

R_{ia}	Thermal resistance between inner and outer pipes in vertical pipe sections(m·K/W)	T_{sur}	geotechnical surface temperature (°C)
r_{eo}	outer radius of outer pipe(m)	$T_{i2}(x,t)$	temperature of the fluid in the inner pipe of the horizontal pipe section(°C)
rei	inner radius of outer pipe(m)	x	axial coordinates of horizontal pipe segments(m)
$(\rho c)_{ep}$	volumetric specific heat capacity of the outer pipe(J/(m²·K))	$T_{a2}(x,t)$	temperature of the fluid in the outer pipe of the horizontal pipe section(°C)
$q_1(z,t)$	heat flow between the outer pipe fluid and the backfill in vertical pipe section(W/m)	L2	length of horizontal pipe section heat exchanger(m)
$q_2(x,t)$	Heat flow between outer pipe fluid and backfill in horizontal pipe sections(W/m)	λ_{g2}	thermal conductivity of backfill in horizontal pipe sections e(W/(m·K))
R_{ab}	Thermal resistance between the annular fluid and the well wall in the horizontal tubing section(mK/W)	$T_b(x,t)$	temperature of the well wall in the horizontal pipe section(°C)

To establish the transient heat transfer equation for the inner and outer pipes of the vertical section and to analyze the heat transfer by using the heat source model of the composite medium column, assuming that the temperature of the fluid in the inner and outer pipes of the vertical section changes only with depth and time, it satisfies the following energy equation:

$$\left[\pi r_{ii}^2 (\rho c)_f + \pi \left(r_{io}^2 - r_{ii}^2 \right)(\rho c)_{ip} \right] \frac{\partial T_{i1}(z,t)}{\partial t}$$
$$= V(t)(\rho c)_f \frac{\partial T_{i1}(z,t)}{\partial z} + \frac{T_{a1}(z,t) - T_{i1}(z,t)}{R_{ia}}, (0 \le z \le L1, t > 0) \tag{1}$$

$$\left[\pi \left(r_{ei}^2 - r_{io}^2 \right)(\rho c)_f + \pi \left(r_{eo}^2 - r_{ei}^2 \right)(\rho c)_{ep} \right] \frac{\partial T_{a1}(z,t)}{\partial t} =$$
$$-V(t)(\rho c)_f \frac{\partial T_{a1}(z,t)}{\partial z} + \frac{T_{i1}(z,t) - T_{a1}(z,t)}{R_{ia}} - q_1(z,t), (0 \le z \le L1, t > 0) \tag{2}$$

The thermal resistance of the fluid in the annulus of a vertical pipe section, which is expressed as:

$$R_{ia} = \frac{1}{2\pi r_{ii} h_i} + \frac{1}{2\pi \lambda_{ip}} \left(\frac{r_{io}}{r_{ii}} \right) + \frac{1}{2\pi r_{io} h_a} \tag{3}$$

The heat flow between the fluid in the outer pipe of a vertical pipe section and the backfill is given by the expression:

$$q_1(z,t) = \frac{T_{a1}(z,t) - T_{eo}(z,t)}{R_{ae}} \tag{4}$$

$$R_{ae} = \frac{1}{2\pi r_{ei} h_a} + \frac{1}{2\pi \lambda_{ep}} \left(\frac{r_{eo}}{r_{ei}} \right) \tag{5}$$

The heat transfer in the backfill and soil of the vertical pipe section is radial one-dimensional heat transfer, then Teo(z,t) is calculated using the composite medium column heat source model:

$$T_{eo}(z,t)\big|_{t=t_n} = T_0(z) + \sum_{j=1}^{n} \left[q_1(z,t)\big|_{t=t_j} - q_1(z,t)\big|_{t=t_{j-1}} \right] G_1(t)\bigg|_{t=t_n - t_{j-1}} \tag{6}$$

Where $G_1(t)$ is the G function of the composite medium column heat source model[X] ;

At the top and bottom of the vertical section of the heat exchanger, the boundary conditions are:

$$\begin{cases} T_{a1}(z_1,t_n)=T_{in}(t),(t>0) \\ T_{i1}(z_M,t_n)=T_{i2}(x_1,t_n),(t>0) \end{cases} \tag{7}$$

At the initial moment, the temperature of both the inner pipe fluid and the outer pipe fluid in the vertical section is equal to the initial temperature of the soil:

$$T_{i1}(z,t)\big|_{t=0} = T_{a1}(z,t)\big|_{t=0} = T_0(z) = T_{sur} + az, (0 \le z \le L1) \tag{8}$$

Secondly, the steady-state heat transfer equations of the inner pipe fluid and the outer pipe fluid in the horizontal section are established, and the heat transfer is analyzed by using the moving line heat source model, assuming that the heat transfer in the borehole of the medium-depth buried pipe is steady-state heat transfer, the heat transfer equations of the inner and outer pipe fluids are:

$$V(t)(\rho c)_f \frac{\partial T_{i2}(x,t)}{\partial x} + \frac{T_{a2}(x,t)-T_{i2}(x,t)}{R_{ia}} = 0, (0 \le x \le L2, t>0) \tag{9}$$

$$-V(t)(\rho c)_f \frac{\partial T_{a2}(x,t)}{\partial x} + \frac{T_{i2}(x,t)-T_{a2}(x,t)}{R_{ia}} - q_2(x,t) = 0, (0 \le x \le L2, t>0) \tag{10}$$

The expression for the heat flow between the well wall and the backfill in the horizontal pipe section is given by:

$$q_2(x,t) = \frac{T_{a2}(x,t)-T_b(x,t)}{R_{ab}} \tag{11}$$

$$R_{ab} = \frac{1}{2\pi r_{ei} h_a} + \frac{1}{2\pi \lambda_{ep}} \ln\left(\frac{r_{eo}}{r_{ei}}\right) + \frac{1}{2\pi \lambda_{g2}} \ln\left(\frac{r_b}{r_{eo}}\right) \tag{12}$$

The temperature of the borehole wall of the horizontal pipe section is calculated analytically using the moving line heat source model combined with the principle of superposition of variable heat flow:

$$T_b(x,t)\big|_{t=t_n} = T_0(L1) + \sum_{j=1}^{n}\left[q_2(x,t)\big|_{t=t_j} - q_2(x,t)\big|_{t=t_{j-1}}\right]G_2(t)\big|_{t=t_n-t_{j-1}} \tag{13}$$

where $G_2(t)$ is the G function of the moving line heat source model[X];

At the top and bottom of the horizontal pipe section of the heat exchanger, the boundary conditions are:

$$\begin{cases} T_{a2}(x,t)\big|_{x=0} = T_{a1}(z,t)\big|_{z=L1}, (t>0) \\ T_{i2}(x,t)\big|_{x=L2} = T_{a2}(x,t)\big|_{x=L2}, (t>0) \end{cases} \tag{14}$$

At the initial moment, the temperature of both the inner pipe fluid and the outer pipe fluid in the horizontal section is equal to the initial temperature of the soil:

$$T_{i2}(x,t)\big|_{t=0} = T_{a2}(x,t)\big|_{t=0} = T_0(L1), (0 \le x \le L2) \tag{15}$$

The nomenclature of which are shown in Table 1. Next, the above heat transfer equation is discretized by segmenting and setting the time step:

Divide the vertical section of the buried pipe into M segments along the axial direction, where the lengths of both the 1st and Mth segments are $\Delta z/2$, and the length of the middle segment is Δz, , the axial coordinate of the mth node $z_m = \Delta z \times (m-1) + \Delta z/2$;

Divide the horizontal section of the buried pipe into K segments along the axial direction, where the lengths of both the 1st and Kth segments are $\Delta x/2$, the length of the middle segment is Δx,, then the axial coordinates of the kth node $x_k = \Delta x \times (k-1) + \Delta x/2$;

Setting the time step Δt, let the total simulation time be t_{tol}, then the number of time segments is N $=t_{tol}/\Delta t$ and $t_n = n\Delta t$;

Discretization of Eq. (1), Eq. (2), Eq. (9), and Eq. (10) and combination of Eqs. (7), (8) and Eqs. (11), (15) give the fluid temperatures of the inner and outer pipes as a function of time and depth.

2.3 Parameter definitions

1. Outlet water temperature T_i (z=0)
2. heat storage capacity $\quad Q_1 = cm\Delta t$
3. heat exchange per meter $\quad Q_{lm} = \dfrac{Q_1}{L_v + L_h}$
4. Initial investment

The outlet water temperature is the temperature of the water coming out of the buried pipe after the heating or cooling water circulates through the buried pipe. This temperature value is affected by a variety of factors, such as buried pipe specifications, soil temperature, and seasonal changes. It is an important parameter that mainly affects the heating or cooling effect of the system, the energy consumption of the buried pipe system, and the service life of the buried pipe. Its expression is: Ti (z=0)

The heat storage capacity of buried pipes is very important for ground source heat pump systems or other geothermal energy recycling systems. The size of heat storage not only affects the effect of building heating or cooling but also affects the heating or cooling capacity, COP value (i.e., energy utilization coefficient of the chiller), and energy efficiency performance of the ground source heat pump system, etc. Its expression is: $Q_1 = cm\Delta t$.

The heat transfer power per meter is the amount of heat transfer that can be accomplished per unit length of the buried pipe. Generally speaking, the extended meter heat transfer power of buried pipe is related to factors such as the thermal conductivity of soil, pipe diameter, and buried depth. According to related research, different types of soil and pipe diameter size have a great influence on the extended meter heat transfer power of buried pipe, which generally can reach $10 \sim 60$ W/(m-K). Its expression is: $Q_{lm} = \dfrac{Q_1}{L_v + L_h}$.

2.4 Model accuracy verification

To validate the developed numerical model, the calculated values were compared with the software-based simulations by Gu et al. [X], where the relevant parameters are shown in Table 1.

The total duration of this simulation is 120 days. The time step is set to be $\Delta t = 600$ seconds, then the number of time segments N=t_{tol}/Δt.

Segment the inner and outer pipe fluids first, dividing the inner pipe fluid 1 into 1251 segments axially along the vertical segment, i.e., M=1251, and the length of the vertical component of the heat exchanger is L=2500 m, then the axial coordinate of the mth node, z_m=L1/(M-1)=2; dividing the inner pipe fluid 1 into 251 segments axially along the horizontal segment, i.e., K=251, and the length of the horizontal part is K=500 m, then the axial coordinate of the kth node x_k=L2/(K-1)=2; similarly, the outer pipe fluid 3 is divided into 1251 segments along the vertical segment axially and 251 segments along the horizontal segment axially.

The discrete equations of the inner and outer pipe fluid temperature fields and their boundary and initial conditions for all moments before the moment t_n are then solved by using the iterative method. Thus, the inner and outer pipe fluid temperatures of each segment of the vertical and horizontal elements at the moment t_n can be calculated, including $T_{i1}(z_1,t_n) \sim T_{i1}(z_M,t_n)$, $T_{a1}(z_1,t_n) \sim T_{a1}(z_M,t_n)$, $T_{i2}(x_1,t_n) \sim T_{i2}(x_K,t_n)$, and $T_{a2}(x_1,t_n) \sim T_{a2}(x_K,t_n)$. Therefore, the temperature distributions of the vertical and horizontal pipes at the moments $t_1 \sim t_N$ can be calculated sequentially.

Under the condition of the ground temperature gradient equal to 0.03°C/m and groundwater seepage in the horizontal pipe section, the comparison of the fluid temperatures calculated with the

developed model in this study for 1, 10, 30, and 120 days with the simulated values carried out by Gu et al. are shown in Figs. 3(A), 3(B), 3(C) and 3(D). Figure 3(A) shows that the maximum error between the fluid temperature calculated in this study and the simulated values is less than 1.3°C and the average relative error is 4%; Figure 3(B) shows that the fluid temperature calculated in this study agrees well with the simulated values, with the maximum deviation of less than 0.7°C and the relative error is even smaller at 3%; Figure 3(C) shows that the fluid temperature calculated in this study agrees the best with the simulated values, with the maximum error of only 0.8°C, and the relative error is only 2%; Figure 3(D) shows that the maximum deviation of the fluid temperature calculated in this study from the simulated value is less than 0.9°C, and the relative error is 3%. It can be seen that the deviation of the fluid temperature calculated in this study from the simulated value is larger in the early stage, while the later stage of the two matches better, but the maximum deviation is less than 1.3°C. Therefore, this study has a certain accuracy in analyzing the fluid temperature distribution under the conditions of the existence of ground temperature gradient and groundwater seepage.
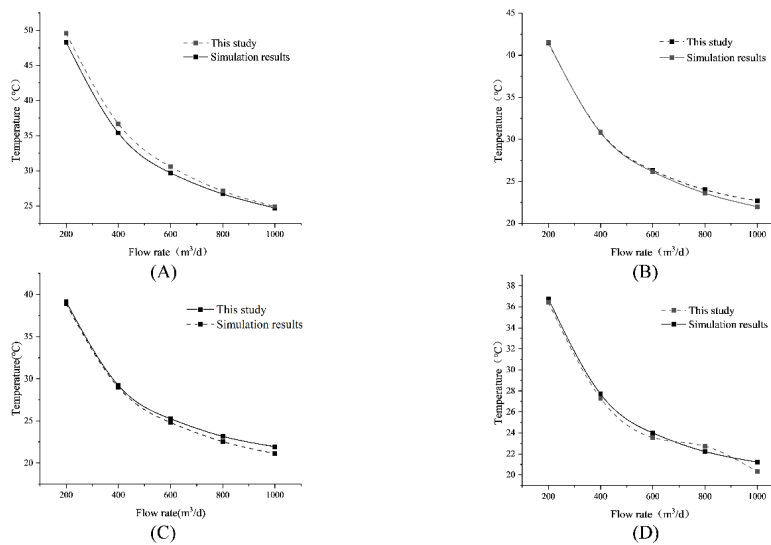
Fig. 3 Model Validation Diagram

3. Result & discussions

This paper examines the factors influencing buried pipe heat exchangers, such as well depth, pipe diameter, soil temperature, thermal conductivity, and groundwater seepage. Using a established model, the study investigates the effects of changing parameters, including a vertical section length of 2500m, a horizontal section length of 500m, a simulation period of 120 days, and control variables. The observations focus on the storage capacity, heat storage, outlet water temperature, and initial investment, optimizing the design of the buried pipe based on the volumes of inner pipe fluid, annular fluid, and outer pipe fluid obtained from the simulation.

Table 2 parameters

parameters	Value
Length of the vertical section of DBHE L1(m)	2500
Length of the horizontal section of DBHE L2(m)	500
Inner radius of inner pipe r_{ii}(m)	0.038
Outer radius of inner pipe r_{io}(m)	0.057
Inner radius of outer pipe r_{ei}(m)	0.08305
Outer radius of outer pipe r_{eo}(m)	0.08995

Borehole radius r_b(m)	0.12225
Thermal conductivity of the inner pipe λ_{ip}(W/m/K)	0.02
Thermal conductivity of the outer pipe λ_{ep}(W/m/K)	40
Thermal conductivity of grout λ_g(W/m/K)	0.8
Thermal conductivity of vertical segments of rock λ_s(m^2/s)	2.27
Thermal diffusivity of a vertical section of rock a_s(m^2/s)	2.11×10^6
Thermal conductivity of horizontal segments of rockλ_{s2}(m^2/s)	2.38
Thermal diffusivity of a horizontal section of rock a_{s2}(m^2/s)	8.41×10^7
Groundwater seepage rate in horizontal section u(m^2/s)	1.91×10^{-7}
Thermal conductivity of fluid λ_f(W/m/K)	0.6
Volumetric specific heat capacity of fluid $(\rho c)_f$(W/m/K)	4.19×10^6
Kinematic viscosity of fluids v(m^2/s)	1.04×10^{-6}
Prandtl number of fluids Pr	7.28
Volume flow rate of fluidV(t) (m^3/s)	2.31×10^{-3}
Inlet fluid temperature T_{in}(t)(°C)	15.0

3.1 Simultaneous change of inner and outer pipe diameters with no change in inner and outer pipe gaps (Option 1)

This subsection uses the simultaneous increase or decrease of the inner and outer pipe diameters and the variation of the temperature at each section point with the length and diameter of the pipe for the medium-depth buried pipe containing horizontal wells at a fixed inlet water temperature of 15°C is shown in Fig. 4. Figure 4 r represents the outer pipe diameter: r1= 0.1399 (m); r2=0.1499 (m); r3=0.1699 (m); r4=0.1799 (m); r5=0.1899 (m); r6=0.1999 (m); r7=0.2099 (m); and r8=0.2199; which represent different outer pipe diameters, respectively. The variation of the heat storage capacity of the buried pipe with the change of pipe diameter is shown in Fig. 5.

Analyzing Figure 4 (A) shows that: the temperature of each section point of the inner tube of the vertical tube section increases with the increase of the sheer tube length, but because of its increase with depth, the temperature difference at the end decreases gradually, the rate of change of the fluid temperature increase slows down with the rise in the length, and the temperature increases with the growth of the inner and outer tube diameter; analyzing Figure 5 (A) shows that the heat storage capacity increases with the increase of the vertical tube length, and increases with the rise of the inner and outer pipe diameter; And when the inner and outer pipe diameter reaches r8 at the same time, the maximum value of heat storage is about 235KW, and the total temperature value is about 39.2°C.

In the horizontal pipe section of the inner pipe, its temperature changes with the length and diameter of the pipe section, as shown in Fig. 4(D). The temperature almost does not change with the increase of the pipe section length but increases with the increase of each pipe diameter; its heat storage capacity changes with the pipe diameter as shown in Fig. 5 (D), and the maximum value of the heat storage capacity is about 236KW, and the maximum value of the temperature is about 39.4°C when the diameter of the inner and outer pipe reaches r8 at the same time.
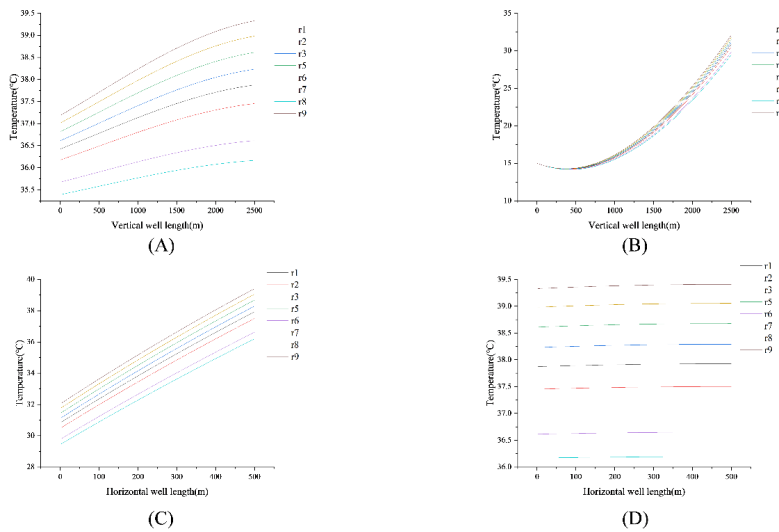
Fig. 4 Temperature variation with simultaneous change of inner and outer pipe diameters
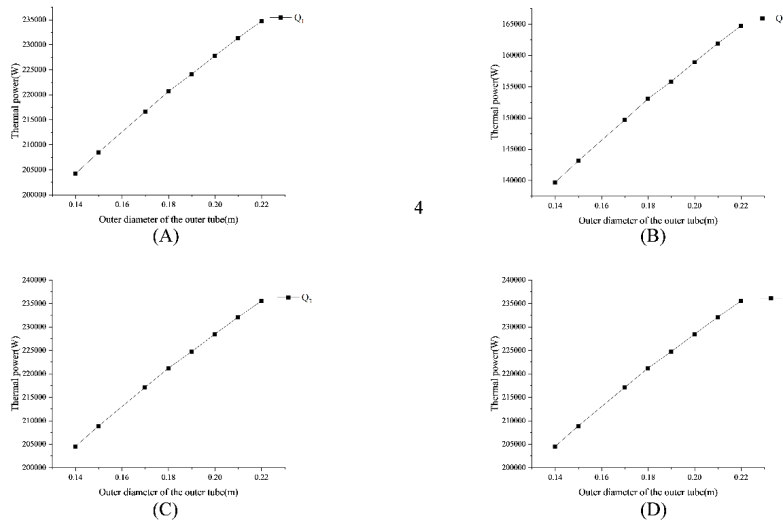
Fig. 5 Variation of heat storage capacity with simultaneous change of inner and outer pipe diameters

3.2 Keep the inner pipe diameter unchanged change the outer pipe diameter (Option 2)

Compared with the simultaneous increase of the inner and outer pipe diameters, only the outer pipe diameter is increased in this subsection, and nine pipe diameters are used for comparison, where r1= 0.1399 (m); r2=0.1499 (m); r3=0.1599 (m); r4=0.1699 (m); r5=0.1799 (m); r6=0.1899 (m); r7=0.1999 (m); r8=0.2099 (m); and r9=0.2199 (m).

Analysis of Figure 6 (A) shows that the vertical pipe section of the inner tube of each section point temperature increases with the increase in the length of the vertical pipe. Still, because of its expansion with the depth, at the end of the temperature difference gradually decreases, the rate of change of the fluid temperature increases with the increase in the length of the gradually slowed down, and the temperature rises with the increase in the outer pipe diameter; analysis of Figure 7 (A) shows that its heat storage increases with the increase in the outer diameter of the pipe. And when the outer pipe diameter reaches r9 storage heat maximum value of about 242KW, the temperature maximum value of about 40.1 ℃.

Figures 6(B) and 7(B) demonstrate the temperature and heat storage capacity variations at different section points along the outer pipe of the vertical section, respectively. The temperature initially

decreases near the shallow position, with the lowest value of 14.32°C at approximately 200m depth when the pipe diameter is r1, and gradually increases with depth.
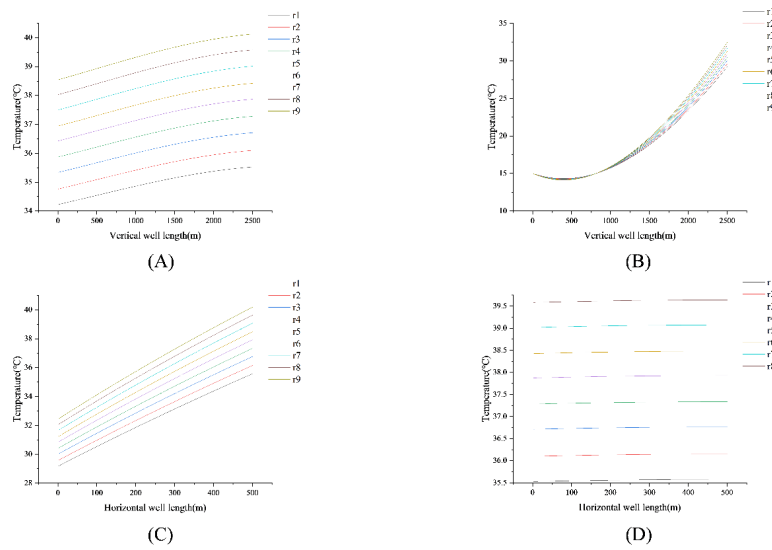
Fig. 6 Variation of temperature with change of outer pipe diameter
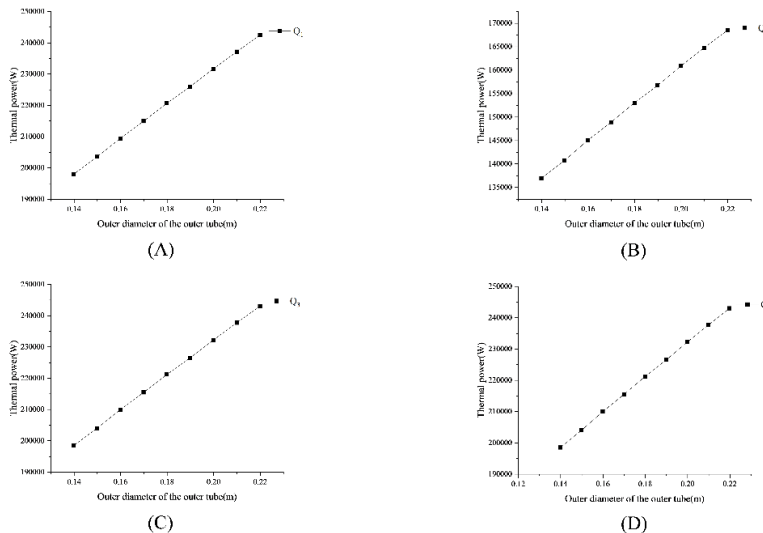
Fig. 7 Variation of heat storage capacity with change in outer pipe diameter

3.3 Keep the outer pipe diameter unchanged change the inner pipe diameter (Option 3)

In this subsection, only the inner pipe diameter is increased and 9 pipe diameters are used for comparison, where r1=0.037 (m); r2=0.042 (m); r3=0.047 (m); r4=0.052 (m); r5=0.057 (m); r6=0.062 (m); r7=0.067; r8=0.072 (m); r9=0.077 (m).

Analyzing Figure 8 (A), it is observed that the temperature of each section point along the inner pipe of the vertical section increases with vertical pipe length. The temperature growth trend varies across different pipe diameters, with the smallest slope observed for r9 and the largest for r1, indicating that temperature growth slope increases with pipe diameter. For pipe lengths below 800m, temperature decreases with increasing inner pipe diameter, while for pipe lengths above 800m, temperature increases with increasing inner pipe diameter. Analyzing Figure 9 (A), it is evident that the heat storage capacity increases with increasing inner pipe diameter. At inner pipe diameter r9, the maximum heat storage value is approximately 225KW, with a maximum temperature value of about 38.3℃.

Figures 8(B) and 9(B) illustrate the temperature and heat storage variations at different cross-section points along the outer pipe of the vertical section, following a similar pattern as the previous

case. Noteworthy differences include the minimum temperature of 14.11°C at pipe diameter r1, gradually increasing with depth, and the minimum temperature of 14.33°C at pipe diameter r9. The inner pipe temperature reaches a maximum of 14.33°C at diameter r9. At the same diameter, the maximum heat storage value is approximately 157 KW, and the maximum temperature value is around 31.31℃.

Next, the temperature and heat storage capacity of the horizontal pipe section are discussed. analyzing Fig. 8(C) and Fig. 9(C), it can be seen that similar to the above scheme, the maximum value of heat storage is about 225 KW when the diameter of the inner pipe reaches r9. The maximum value of the temperature is about 38.35 °C.

Analysis of Fig. 8 (D) and Fig. 9 (D) shows that, similar to the above scheme, when the diameter of the inner tube reaches r9, the heat storage capacity and temperature of the outer tube reaches the maximum value, and the maximum value of the heat storage capacity is about 225KW and the maximum value of the temperature is about 38. 35°C.
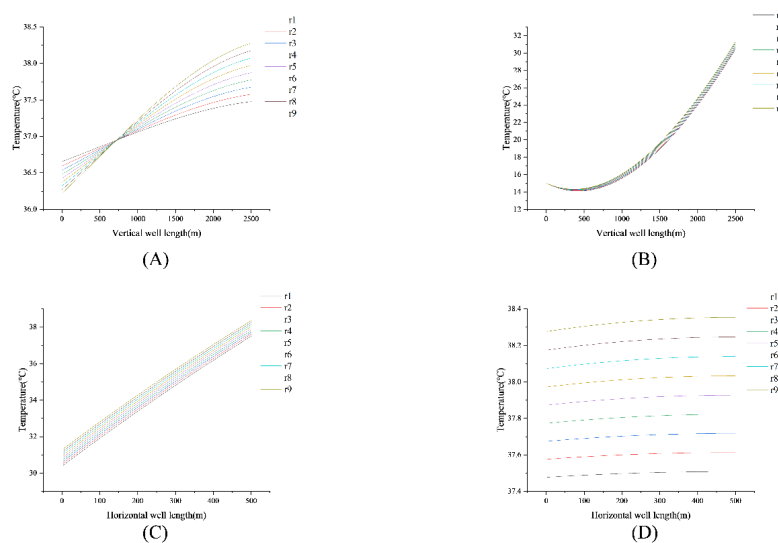
Fig. 8 Variation of temperature with inner tube diameter

3.4 Economic analysis

After the actual investigation, the material used in the pipeline is mostly Pe material, and its price per meter is related to the size of the inner and outer pipe diameter, the initial investment of a vertical section of 2500m and a horizontal section of 500m long cased buried pipe under different pipe diameter conditions includes the investment in pipeline and the investment in pumps, which includes the cost of the vertical section and the horizontal section of the pipeline and the cost of pumps, which include the cost of heat pumps and circulating water pumps. The investment of heat pump is 24×10⁴RMB[X], and the rest of the cost is shown in the following table.
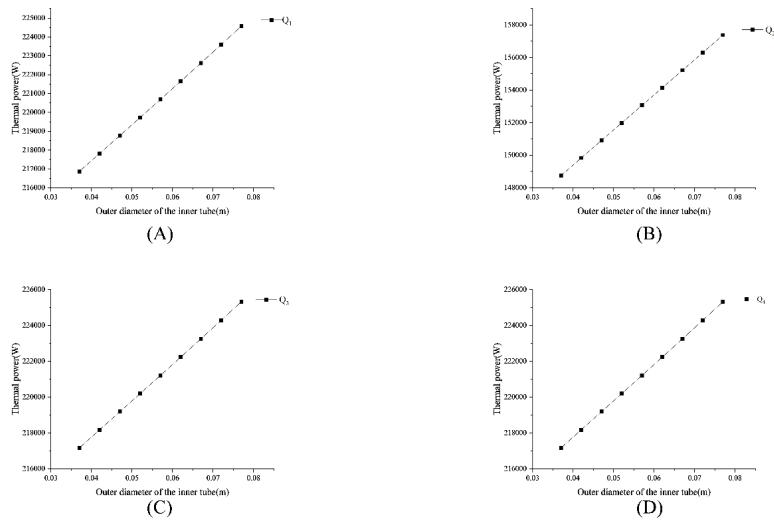
Fig. 9 Variation of heat storage capacity with variation of inner pipe diameter

Table 3 Simultaneous change of inner and outer pipe diameters with constant inner and outer pipe gap

	Vertical well Cost($\times 10^4$RMB)	Horizontal well Cost($\times 10^4$RMB)	Injection pump Cost($\times 10^4$RMB)
r1	16.3	3.3	19.7
r2	19.3	3.9	19.7
r3	22.4	4.5	19.6
r4	29.5	5.9	19.6
r5	33.7	6.7	19.6
r6	37.7	7.5	19.6
r7	42.4	8.5	19.6
r8	47	9.4	19.6

Table 4 Changing the outer pipe diameter by keeping the inner pipe diameter unchanged

	Vertical well Cost($\times 10^4$RMB)	Horizontal well Cost($\times 10^4$RMB)	Injection pump Cost($\times 10^4$RMB)
r1	21.2	4.2	19.7
r2	23.1	4.6	19.6
r3	25.1	5.0	19.6
r4	27.3	5.5	19.6
r5	29.5	5.9	19.6
r6	32.0	6.4	19.6
r7	34.4	6.9	19.6
r8	37.2	7.4	19.6
r9	40.0	8.0	19.6

Table 5 Changing the inner pipe diameter by keeping the outer pipe diameter unchanged

	Vertical well Cost($\times 10^4$RMB)	Horizontal well Cost($\times 10^4$RMB)	Injection pump Cost($\times 10^4$RMB)
r1	24.7	4.9	19.7
r2	25.7	5.1	19.7
r3	26.8	5.4	19.6
r4	28.1	5.6	19.6
r5	29.5	5.9	19.6
r6	31.2	6.2	19.6
r7	32.7	6.5	19.6
r8	34.7	6.9	19.6
r9	36.5	7.3	19.7

The sum of the initial investment for the above three scenarios is shown below, where the orange color represents the cost of the circulation pump, the light blue color represents the cost of the horizontal section of piping, and the dark blue color represents the cost of the vertical section of piping.
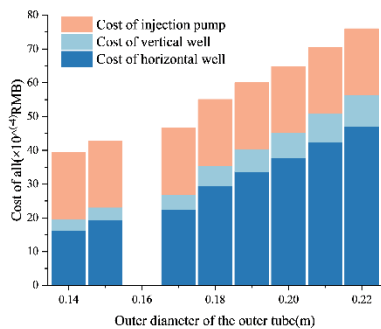
Fig. 10 Total investment in Option 1   Fig. 11 Total investment in Option 2   Fig. 12 Total investment in Option 3
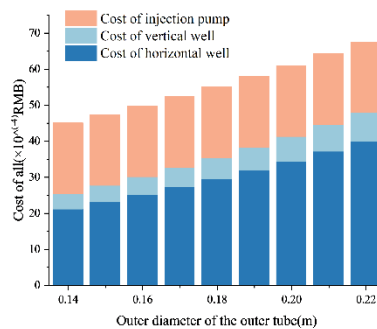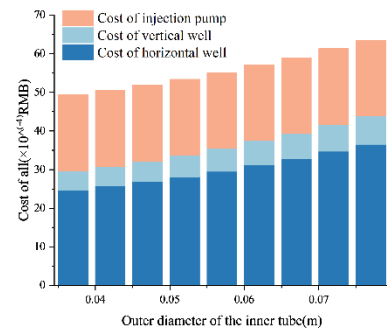
Figure 10 shows that the total investment for Scheme 1 increases with pipe diameter, reaching a maximum of 56.4×104 RMB. The growth trend differs, with r1-r2, r3-r4, r5-r6, and r7-r8 showing larger increases compared to r2-r3, r4-r5, and r6-r7. Additionally, the investment in the pipeline increases gradually with pipe diameter, with r3-r4 exhibiting a sudden increase and reaching a maximum of 1.32.

In Figure 11, the total investment for Scheme II increases with pipe diameter, reaching a maximum of 48.0×104 RMB. The growth trend varies, with r1-r2, r3-r4, r5-r6, and r7-r8 showing a slower increase compared to r2-r3, r4-r5, and r6-r7. The investment in the pipeline increases gradually with pipe diameter, with a maximum value of 1.05.

Figure 12 depicts that the total investment for Scheme III increases with pipe diameter, reaching a maximum of 43.8×104 RMB. The growth trend differs, with r1-r2, r3-r4, r5-r6, and r7-r8 exhibiting larger increases compared to r2-r3, r4-r5, and r6-r7. The investment in the pipeline gradually increases with pipe diameter, with fluctuations at a later stage, particularly with r6-r7 showing the largest increase of 1.06.

3.4 Discuss

This paperbased on the same simulation background: the same ground temperature gradient, the same groundwater seepage velocity, and the same fluid velocity, change the inner and outer pipe diameters of the cased underground pipe and observe the changes of its fluid temperature distribution and heat storage, in addition to the investigation, prediction, and analysis of the initial investment of the underground pipe, and get the following conclusions:

Conclusion 1: the internal and external pipe clearance is unchanged at the same time Increasing the internal and external pipe diameter will make he vertical pipe section and the horizontal pipe section of the temperature with the increase in pipe diameter and increase. And the heat storage capacity of both vertical pipe section and horizontal pipe section increases with the increase of pipe diameter, but the slope fluctuates.

Conclusion 2: The effect of constant inner pipe diameter and increasing outer pipe diameter on temperatures in the vertical pipe section is similar to the previous case, but with a larger trend of change and higher outlet temperature. Changing the diameter of the pipe section has a greater impact on the shallow and deep temperatures of the inner pipe in the vertical section, while the outer pipe temperature in the vertical section and both inner and outer pipe temperatures in the horizontal section show relatively minor changes. Increasing the pipe diameter in both scenarios enhances the heat storage capacity in both vertical and horizontal pipe sections.

Conclusion 3: According to the initial investment of the system can be seen, the initial investment of the above three programs increased with the increase in pipe diameter, but the pipeline increasing trend: program one is greater than program two is greater than program three, and the total initial investment is also program one is greater than program two is greater than program three.

And the above conclusions can be seen in program two temperature increase degree is greater than in program three, and the initial investment in program one is more expensive than in program two, so the above program two is more reasonable. In the programs r3, r5, r7, and r9, investment is small, and the temperature increase.

4. Conclusion

This paper focuses on the influence of inner and outer pipe diameters on the temperature distribution and heat storage capacity of buried pipe in the buried pipe heat exchange system with a horizontal well, innovatively establishes a semi-analytical model with a horizontal well, and changes the inner and outer pipe diameters and conducts simulation and analysis, discusses the temperature distribution and heat storage capacity of the buried pipe with horizontal well and comprehensively considers the initial investment of the buried pipe. It is concluded that all the above three options will make the buried pipe temperature increase, heat storage capacity increase, and option three increase the trend of the smallest; and then consider the economy of its investment in option two is small, the temperature increase is large.

Overall, this paper considers the effects of different pipe diameters of buried pipe on the temperature distribution and heat storage capacity of buried pipe. Compared with the unoptimized ones, it improves the temperature and heat storage capacity and makes it a relatively small increase in cost, and the results of the study are instructive for the design of the deep and medium-cased buried pipe containing horizontal wells. However, many factors have not been considered, including the ratio of vertical to horizontal pipe sections, fluid flow rates, and different geotechnical thermophysical properties.

In further studies, the ratio of vertical and horizontal pipe sections, the effect of fluid flow, and different geotechnical thermophysical properties can be re-modeled, taking into account, and all of them can be considered in the optimal design of buried pipes containing horizontal pipes.

References

[1] Ferda Halicioglu, Natalya Ketenci. Output, renewable and non-renewable energy production, and international trade: evidence from EU-15 countries. Energy. Vol. 159 (2018), p. 995-1002.

[2] Benjamin K. Sovacool. Contestation, contingency, and justice in the Nordic low-carbon energy transition. Energy Policy. Vol. 102 (2017), p. 569-582.

[3] Shyi-Min Lu. A global review of enhanced geothermal system (EGS), Renew. Sustain. Energy Reviews. Vol. 81 (2018), p. 2902-2921.

[4] John W. Lund, John W. Lund. Direct utilization of geothermal energy 2020 worldwide review - ScienceDirect. Geothermics. Vol. 90 (2021) No. 101915.

[5] Aneta Sapinska-Sliwa, Marc A. Rosen, Andrzej Gonet, et al. Deep Borehole Heat Exchangers — A Conceptual and Comparative Review. International Journal of Air-Conditioning and Refrigeration. Vol. 24 (2015) No. 01, p. 19-25.

[6] Xu-Wei Wang, Xu-Wei Wang, Shui-Long Shen, et al. Distribution characteristics and utilization of shallow geothermal energy in China. Energy and Buildings. Vol. 299 (2020) No. 110479.

[7] Jiewen Deng, Qingpeng Wei, Shi He, et al. Simulation Analysis on the Heat Performance of Deep Borehole Heat Exchangers in Medium-Depth Geothermal Heat Pump Systems. Energies. Vol. 13 (2020), p. 1-28.

[8] Alimonti, C, Soldo, E, Bocchetti, D, et al. The wellbore heat exchangers: a technical review. Renew. Energy. Vol. 123 (2018), p. 353-381.

[9] M. Soltani, Moradi Kashkooli, F, A.R. Dehghani-Sanij, et al. A comprehensive review of geothermal energy evolution and development. International Journal of Green Energy. Vol. 16 (2019), p. 971-1009.

[10] Yongqaing Luo, Hongshan Guo, Forrest Meggers, et al. Deep coaxial borehole heat exchanger: analytical modeling and thermal analysis. Energy. Vol. 185 (2019), p. 1298–1313.

[11] Henrik Holmberg, José Acuña, Erling Næss, et al. Thermal evaluation of coaxial deep borehole heat exchangers. Renewable Energy. Vol. 97 (2016), p. 65-76.

[12] Jiewen Deng, Shi He, Qingpeng Wei, et al. Field test and optimization of heat pumps and water distribution systems in medium-depth geothermal heat pump systems. Energy and Buildings. Vol. 209 (2020), p. 1-14.

[13] Stefano, Morchio, Marco, et al. Thermal modeling of deep borehole heat exchangers for geothermal applications in densely populated urban areas - ScienceDirect. Thermal Science and Engineering Progress. Vol. 13 (2023) No. 100363.

[14] Jiuchen Ma, Qian Jiang, Qian Jiang, et al. Effect of groundwater forced seepage on heat transfer characteristics of borehole heat exchangers. Geothermal Energy. Vol. 9 (2021) No. 11.

[15] B Badenes, MNM Pla, T Magraner, et al. Theoretical and Experimental Cost–Benefit Assessment of Borehole Heat Exchangers (BHEs) According to Working Fluid Flow Rate. Energies. Vol. 13 (2020) No. 4925.

[16] Zhang, Changxing, Hu, Songtao, Liu, Yufeng, et al. Optimal design of borehole heat exchangers based on hourly load simulation. Energy. Vol. 116 (2016), p. 1180-1190.

[17] Lazaros Aresti, Paul Christodoulides, Georgios Florides. A review of the design aspects of ground heat exchangers. Renewable and Sustainable Energy Reviews. Vol. 92 (2018), p. 757-773.

[18] Changlong Wang, Xin Wang, Jinli Lu, et al. A semi-analytical heat transfer model for deep borehole heat exchanger considering groundwater seepage. International Journal of Thermal Sciences. Vol. 175 (2022) No. 107465.

[19] Dingshan Du, Yongqiang Li, Kaipeng Wang, et al. Experimental and numerical simulation research on heat transfer performance of coaxial casing heat exchanger in 3500m-deep geothermal well in Weihe Basin. Geothermics. Vol. 109 (2023) No. 102658.

[20] Asal Bidarmaghz, Guillermo A. Narsilio. Is natural convection within an aquifer a critical phenomenon in deep borehole heat exchangers' efficiency?. Applied Thermal Engineering. Vol. 212 (2022) No. 118450.

[21] Hu, Jinzhong. An improved analytical model for vertical borehole ground heatexchanger with multiple-layer substrates and groundwater flow. Applied energy. Vol. 202 (2017), p. 537-549.

[22] Xing Zou, Peng Pei, DingYi Hao, et al. Numerical analysis of the effect of different soil types and moisture content on the heat transfer performance of horizontally buried pipes. Coal Geology & Exploration. Vol. 6 (2021), p. 221-229.

[23] WanLi Wang: Evaluation of Heat Transfer Characteristics and Heat Transfer Efficiency of Vertical Submerged Pipes in Layered Stratigraphy (doctor, China University of Geosciences, China 2019). p.1-114.

[24] Shui Huang, JianKai Dong, Ji Li, et al. Heat extraction characteristics of medium-depth buried tube heat exchanger in different operation modes. Gas & Heat. Vol. 3 (2022), p. 1-5.